2017

Emissions of Glyoxal and Other Carbonyl Compounds from Agricultural Biomass Burning Plumes Sampled by Aircraft

Kyle J. Zarzana
University of Colorado Boulder

Kyung-Eun Min
Gwangju Institute of Science & Technology

Rebecca A. Washenfelder
University of Colorado Boulder

Jennifer Kaiser
Harvard University

Mitchell Krawiec-Thayer
University of Wisconsin - Madison

See next page for additional authors

Authors
Kyle J. Zarzana, Kyung-Eun Min, Rebecca A. Washenfelder, Jennifer Kaiser, Mitchell Krawiec-Thayer, Jeff Peischl, J. Andrew Neuman, John B. Nowak, Nicholas L. Wagner, William P. Dubè, Jason M. St. Clair, Glenn M. Wolfe, Thomas F. Hanisco, Frank N. Keutsch, Thomas B. Ryerson, and Steven S. Brown

Environmental Science & Technology

Article

pubs.acs.org/est

Emissions of Glyoxal and Other Carbonyl Compounds from Agricultural Biomass Burning Plumes Sampled by Aircraft

Kyle J. Zarzana,[†,‡] Kyung-Eun Min,[†,‡,#] Rebecca A. Washenfelder,[†,‡] Jennifer Kaiser,[¶,⊗] Mitchell Krawiec-Thayer,[¶] Jeff Peischl,[†,‡] J. Andrew Neuman,[†,‡] John B. Nowak,[†,‡,Δ] Nicholas L. Wagner,[†,‡] William P. Dubè,[†,‡] Jason M. St. Clair,[§,∥] Glenn M. Wolfe,[§,∥] Thomas F. Hanisco,[§] Frank N. Keutsch,[¶,▽] Thomas B. Ryerson,[†] and Steven S. Brown*[,†,⊥]

[†]Chemical Sciences Division, NOAA Earth System Research Laboratory (ESRL), Boulder, Colorado 80305, United States

[‡]Cooperative Institute for Research in Environmental Sciences, University of Colorado Boulder, Boulder, Colorado 80309, United States

[¶]Department of Chemistry, University of Wisconsin−Madison, Madison, Wisconsin 53706, United States

[§]Atmospheric Chemistry & Dynamics Laboratory, NASA Goddard Space Flight Center, Greenbelt, Maryland 20771, United States

[∥]Joint Center for Earth Systems Technology, University of Maryland Baltimore County, Baltimore, Maryland 21250, United States

[⊥]Department of Chemistry & Biochemistry, University of Colorado Boulder, Boulder, Colorado 80309, United States

Supporting Information

ABSTRACT: We report enhancements of glyoxal and methylglyoxal relative to carbon monoxide and formaldehyde in agricultural biomass burning plumes intercepted by the NOAA WP-3D aircraft during the 2013 Southeast Nexus and 2015 Shale Oil and Natural Gas Nexus campaigns. Glyoxal and methylglyoxal were measured using broadband cavity enhanced spectroscopy, which for glyoxal provides a highly selective and sensitive measurement. While enhancement ratios of other species such as methane and formaldehyde were consistent with previous measurements, glyoxal enhancements relative to carbon monoxide averaged 0.0016 ± 0.0009, a factor of 4 lower than values used in global models. Glyoxal enhancements relative to formaldehyde were 30 times lower than previously reported, averaging 0.038 ± 0.02. Several glyoxal loss processes such as photolysis, reactions with hydroxyl radicals, and aerosol uptake were found to be insufficient to explain the lower measured values of glyoxal relative to other biomass burning trace gases, indicating that glyoxal emissions from agricultural biomass burning may be significantly overestimated. Methylglyoxal enhancements were three to six times higher than reported in other recent studies, but spectral interferences from other substituted dicarbyonyls introduce an estimated correction factor of 2 and at least a 25% uncertainty, such that accurate measurements of the enhancements are difficult.

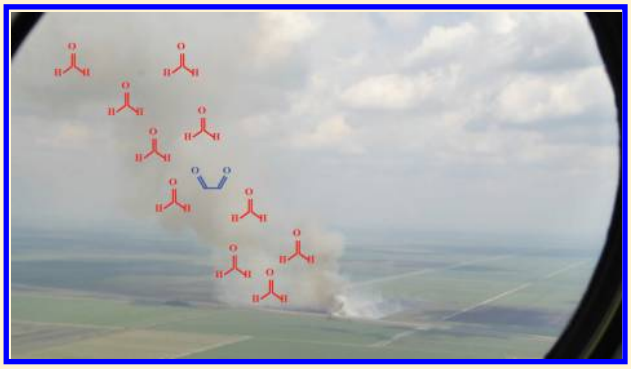

INTRODUCTION

Biomass burning is a large source of reactive gases and particulate matter that can have major effects on local and regional atmospheric chemistry and human health.[1,2] The emissions from biomass burning form a complex mixture of species that can change over the duration of the fire and undergo further chemical reactions as emissions are transported downwind. Accurate measurements of fire emissions and fire plume composition after aging are needed, but the data are lacking for many species.[3,4]

Carbonyl compounds such as formaldehyde (HCHO), glyoxal (CHOCHO), and methylglyoxal (CH_3COCHO) are emitted in large amounts by fires,[3−5] and these compounds can affect numerous atmospheric processes. Their photolysis can form radicals that affect hydroxyl radical (OH) concentrations and ozone (O_3) formation,[6−8] and the heterogeneous uptake of CHOCHO and CH_3COCHO can contribute to the formation of secondary organic aerosol and brown carbon.[9−11] Additionally, both CHOCHO and HCHO can be detected from satellites,[12,13] and the ratio of those two species has been used as a tracer for the oxidation of other volatile organic compounds.[14,15]

CHOCHO mixing ratios in ambient air typically do not exceed 100−200 pptv,[15−17] but in highly polluted urban areas[18,19] or in biomass burning plumes such as those observed

Received: July 11, 2017
Revised: September 19, 2017
Accepted: September 25, 2017
Published: October 4, 2017

DOI: 10.1021/acs.est.7b03517
Environ. Sci. Technol. 2017, 51, 11761−11770

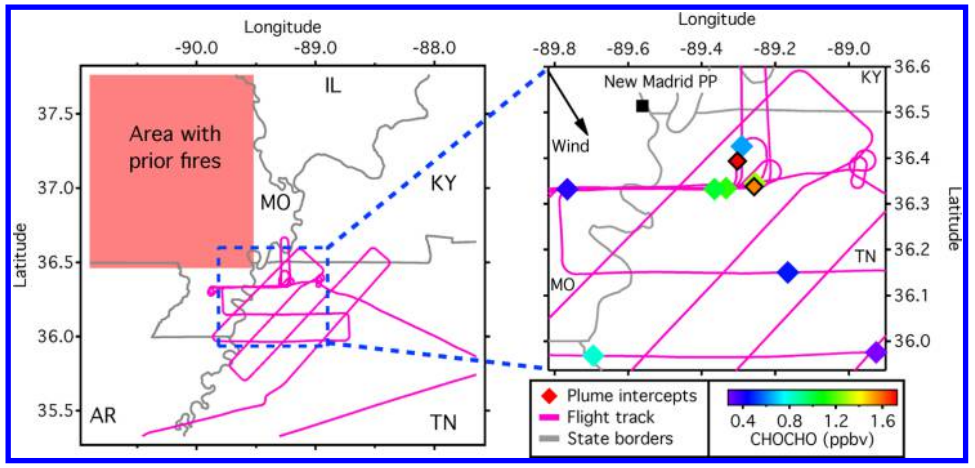

Figure 1. General location of the flight on the night of 2/3 July 2013 (a). The red box indicates the area where numerous fires occurred in the weeks prior to the flight. An expanded view of the area inside the blue dashed lines is shown in panel b, with plume intercept locations and flight track from the relevant portion of the flight. The black marker is the New Madrid power plant, and the plume intercept markers are colored by CHOCHO mixing ratios. CHOCHO mixing ratios outside the plumes were below the detection limit. The two markers outlined in black are the plumes intercepted at 20:55 and 21:46 CDT.

here, mixing ratios may be several parts per billion. However, to the best of our knowledge there are only two previous reports of the actual emission rates of CHOCHO from wood and foliar burning fires, both conducted in the laboratory.[20,21] The data from these two studies suggest that CHOCHO emissions from the studied fuels are roughly equal to those from HCHO on a molar basis. These studies in turn have been used to parametrize emissions in global models, which find biomass burning to be a significant contribution (12%) to the global CHOCHO budget.[22] However, only a limited number of fuels were examined, and the reported emission factors were averaged over the whole fire, and thus may not capture changes in emission rates due to changes in the stage of the fire (e.g., flaming versus smoldering).

Both laboratory studies used a method where CHOCHO was collected on cartridges coated with 2,4-dinitrophenylhydrazine (DNPH), which reacts with carbonyls to form carbonyl DNP hydrazones. The derivatized products were separated using high-performance liquid chromatography (HPLC) and quantified by measuring the absorption at 360 nm. However, this method is now known to have interferences from species such as nitrogen dioxide (NO_2) and O_3.[23,24] Proton-transfer-reaction mass spectrometry (PTR-MS) has been used to quantify many fire emission compounds including HCHO and CH_3COCHO,[4,25] but CHOCHO decomposes to HCHO in PTR-MS instruments,[26] so CHOCHO cannot be quantified using this method, and CHOCHO could be a significant interference for PTR-MS measurements of HCHO.

CHOCHO can also be detected by either using laser-induced phosphorescence (LIP)[14,27] or by taking advantage of CHOCHO's relatively large and structured visible absorption cross section near 455 nm.[18,28] When the latter method is used with cavity enhanced techniques such as broadband cavity enhanced spectroscopy (BBCES)[17,29] or cavity enhanced differential optical absorption spectroscopy (CE-DOAS),[30] sensitive and rapid detection of CHOCHO is possible, even in the presence of species with overlapping absorption features such as NO_2 and CH_3COCHO. BBCES instruments are also compact enough to be deployed on research aircraft to investigate emissions in the field instead of only in laboratory settings. In this study, we use measurements of CHOCHO from an airborne BBCES instrument to derive CHOCHO enhancements from several small agricultural fires in the summertime Southeast United States.

INSTRUMENTATION AND METHODS

Instruments. Data for this study were acquired on the NOAA WP-3D aircraft during the 2013 Southeast Nexus (SENEX, https://www.esrl.noaa.gov/csd/projects/senex) and the 2015 Shale Oil and Natural Gas Nexus (SONGNEX, https://www.esrl.noaa.gov/csd/projects/songnex) field campaigns. Full details of the SENEX payload are given in Warneke et al.,[31] and while the gas phase measurements during SONGNEX were similar, only limited particle phase measurements were available during that campaign.

All the instruments used for this study have been described previously, so only brief descriptions will be provided here. CHOCHO was measured using the NOAA Airborne Cavity Enhanced Spectrometer (ACES).[17] Light from an LED centered at 455 nm was coupled into a high finesse optical cavity, and the wavelength resolved intensity of light between 438 and 470 nm exiting the cavity was measured using a spectrometer and CCD camera. The resulting spectra were fit using standard spectral fitting routines contained in the DOASIS software package.[32,33] These fitting routines use literature cross sections for CHOCHO, CH_3COCHO, NO_2, the oxygen dimer, O_4, and water vapor to retrieve the concentrations of those species. This fitting method works best for species whose cross sections have large differential structure, such as CHOCHO and NO_2, and performs less well when the cross sections are unstructured, as is the case for CH_3COCHO. However, the concentration of CH_3COCHO in the fire plumes was often high enough to make a retrieval possible. An example fit is shown in the supplement (Figure S1). Due to the relatively low ambient concentrations of CHOCHO, data previously had been reported at 5 s intervals, with a 2σ detection limit of 35 pptv,[17] and a spatial resolution of 500 m at typical aircraft speeds. CHOCHO mixing ratios in the plumes often exceeded 500 pptv, and the plumes exhibited a sharp temporal structure, so the data were reported at 1 s intervals, with a 2σ detection limit of 80 pptv. For CH_3COCHO, the 1 s detection limit calculated by running

DOI: 10.1021/acs.est.7b03517
Environ. Sci. Technol. 2017, 51, 11761−11770

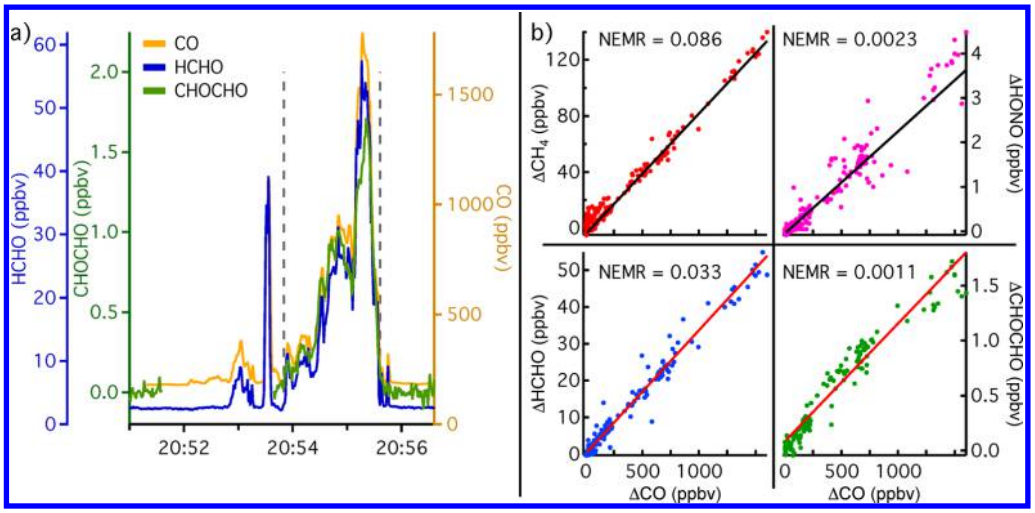

Figure 2. Time series of CHOCHO, HCHO, and CO for the plume intercepted at 20:55 CDT on 2 July 2013 (a). Also shown are plots of ΔCH_4, ΔHONO, ΔHCHO, and ΔCHOCHO against ΔCO (b).

the retrieval on clean zero air (i.e., air without any absorbers) is ~2 ppbv, with an uncertainty of at least 30%, in agreement with previous work.[30] However, for weak, diffuse absorbers such as CH_3COCHO the detection limit in fire plumes is potentially worse due to the presence of strong absorbers such as NO_2 and potentially interfering species such as biacetyl.

All other species were measured at 1 s intervals. Carbon monoxide (CO) was measured using vacuum ultraviolet fluorescence.[34] HCHO was measured with the NASA In-Situ Airborne Formaldehyde instrument, which uses laser-induced fluorescence.[35] Methane (CH_4) and carbon dioxide (CO_2) were measured using a Picarro 1301-m infrared wavelength scanned cavity ring down spectrometer.[36] Nitrous acid (HONO) was measured using an iodide chemical ionization mass spectrometer.[37] ACES is also capable of measuring HONO, but the mass spectrometer data showed higher precision and are used in the following analysis. Sulfur dioxide (SO_2) was measured using pulsed UV fluorescence.[38] Particle size distributions were measured using an ultra high sensitivity aerosol spectrometer (UHSAS).[39] The optical growth of particles due to water uptake from 20% RH to 90% RH (fRH(90%,20%)) was measured using a multichannel cavity ring-down instrument.[40] Black carbon was measured with a single particle soot photometer (SP2).[41] The last two instruments were only included on the SENEX payload, and were not available for SONGNEX.

Plume Analysis. Fire plumes were identified by large and correlated enhancements in fire tracers such as CHOCHO, HCHO, CO, and black carbon. A total of 17 plumes with significant (>200 pptv) CHOCHO enhancements were identified. We did not observe any fire plumes without CHOCHO. The majority of the plumes were intercepted during the SENEX campaign on the night of 2/3 July 2013 in the vicinity of New Madrid, MO (36.588 N, 89.535 W), when a total of ten intercepts were performed. The general region of the flight, as well as the flight track and plume intercept locations are shown in Figure 1. All plume intercepts occurred in darkness at least 25 min after sunset (20:15 CDT). Large (>1 ppbv) enhancements in HONO were observed in the fire plumes, which, given the short time since sunset, implies that the plumes were at most only a few hours old. No major fires were reported in the local news, and no fires were found in the Fire INventory from NCAR (FINN) database[42] or in the US Department of Agriculture (USDA) Active Fire Mapping Program database[43] on 2/3 July 2013 within 100 km of the intercepts. Numerous fires were found in the FINN database near New Madrid in the 2 weeks before and after the flight, the majority of them northwest of the town (red highlighted area in Figure 1a), and it is likely that the intercepted plumes originated from the same general area. The locations of these fires corresponded to crop fields, and it is likely that the fires intercepted by the WP-3D were also small agriculture fires. Based on data from the USDA CropScape database, the main crops grown upwind of the intercepts were soybeans, corn, and cotton.[44]

Five additional intercepts occurred during SENEX on four different daytime flights. During SONGNEX, two plumes were intercepted during the day, one in Florida and the other in Oklahoma. The FINN database had two fires at roughly the corresponding time and less than 10 km upwind of the Florida intercept. However, no fires were reported within 100 km of the other daytime intercepts. Details on all plume intercepts are given in the tables in the supplement. The fuel being burned in Florida was most likely sugar cane, while the dominant vegetation types near the Oklahoma intercept were grass and winter wheat.[44]

For each intercept, a normalized excess mixing ratio (NEMR),

$$\mathrm{NEMR} = \frac{\Delta X}{\Delta \mathrm{CO}} = \frac{X_{\mathrm{fire}} - X_{\mathrm{bkg}}}{\mathrm{CO}_{\mathrm{fire}} - \mathrm{CO}_{\mathrm{bkg}}} \quad (1)$$

was calculated for CHOCHO, CH_3COCHO, HCHO, CH_4, and HONO. Since the plume ages are not accurately known, we do not interpret the observed enhancement ratios calculated in eq 1 as emission ratios.[3] While NEMRs are usually normalized to CO, we have also calculated NEMRs for CHOCHO and CH_3COCHO normalized to HCHO for comparison with the previous literature.[20,21] In addition to NEMRs, the modified combustion efficiency (MCE)[45]

$$\mathrm{MCE} = \frac{\Delta \mathrm{CO}_2}{\Delta \mathrm{CO}_2 + \Delta \mathrm{CO}} \quad (2)$$

DOI: 10.1021/acs.est.7b03517
Environ. Sci. Technol. 2017, 51, 11761−11770

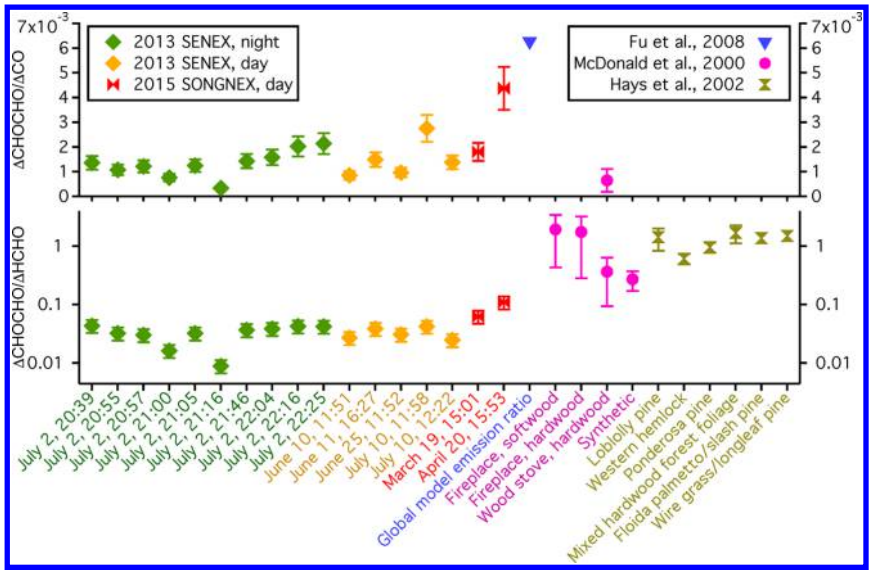

Figure 3. CHOCHO NEMRs determined in this study for the 2013 SENEX and 2015 SONGNEX field projects and literature emission ratios. Ratios against CO are shown in the top, and ratios against HCHO are shown in the bottom. The times for the intercepts are local times.

was calculated for each plume in a similar manner in order to determine the stage of the fire (flaming or smoldering) and examine whether the fire stage affected emissions.

Average background concentrations immediately before and after each plume were calculated and linearly interpolated during the time of the intercept. In several instances one of the background periods was not at the same altitude as the plume intercept. For these plumes, no linear interpolation was performed, and instead the background concentration at the plume altitude was used to represent the background within the plume. While the instruments used are stable with changes in pressure, data that were not at the same altitude as the background were not used in the analysis to avoid any potential artifacts caused by background variations with altitude. For any given plume, the variations in the backgrounds for the different species were significantly less than the enhancements, and did not affect the retrieved NEMR. The background mixing ratio for each species was then subtracted from the plume mixing ratio to give the excess mixing ratio, ΔX. The excess mixing ratio for species X was then plotted against the excess mixing ratio for CO or HCHO, and the slope of the linear orthogonal distance regression was taken as the NEMR. The time series of CHOCHO, HCHO, and CO for the plume intercepted at 20:55 CDT on 2 July 2013, as well as sample correlation plots, are shown in Figure 2.

Roughly half of the plumes intercepted on the night of 2/3 July 2013 were potentially downwind of the New Madrid coal-fired electric power plant (black marker in Figure 1b), and while emissions from the plant could bias the NEMRs reported here, the characteristics of these intercepts suggests that this is not the case. The plume from the plant was intercepted three times when it was not mixed with fire plumes, twice during the night of July 2/3, and once during the day on July 8. As expected, no enhancements in HCHO were observed during these intercepts. The ACES instrument was zeroing during the night intercepts of the power plant plume, but no CHOCHO enhancements were observed during the day. Based on distance and wind speed, the daytime plume was intercepted approximately 45 min after emission, significantly shorter than the expected CHOCHO lifetime of several hours.[46] The plant does emit CO, but the CO enhancements observed in the power plant plume intercepts were ∼100 ppbv, significantly smaller than the enhancements of over 1000 ppbv observed in the fire plumes. The NEMRs relative to CO will be affected at most by 10%, but the MCE might be biased high by the emissions of CO_2 from the plant. SO_2 data were not reported in the fire plumes due to potential interferences from fluorescing hydrocarbons present in biomass burning emissions and thus cannot be used to separate out any influence from the power plant. However, in the biomass burning plumes CO, CO_2, and HCHO were all well correlated, which was not the case in the two power plant plumes. Additionally, the CO outside of the fire and power plant plumes was essentially the same both close to and far away from the power plant, indicating that the power plant had a minimal influence on the background levels of CO.

Based on the measurement uncertainties for CO (5%), HCHO (10%), and CHOCHO (15%), we assign a conservative uncertainty of 20% to the CHOCHO to CO NEMRs and 25% to the CHOCHO to HCHO NEMRs by linear addition of the uncertainties in the measurements.

RESULTS AND DISCUSSION

Validation of Method Using Other Species. NEMRs for CH_4, HONO, and HCHO were calculated for each plume and are shown in the supplement (Figure S2), along with the range of values from the literature. With the exception of the daytime HONO values, all retrieved NEMRs were within the range of previously reported values. Except for one plume (discussed below), HONO mixing ratios in the daytime plumes were below 100 pptv and consistent with known emission sources or gas-phase production from OH+NO.[37] The retrieved HCHO to CO NEMRs are on the high end of previous laboratory measurements,[4] but are consistent with HCHO emissions from agricultural fires observed in the southeast US from the NASA DC-8 in September 2013 (average of 0.038).[5]

Modified Combustion Efficiencies. MCE values for the 17 plumes ranged between 0.91 and 0.97. An MCE of 0.9 indicates that the fire was half smoldering and half flaming,[3] so the fires observed during these two campaigns were generally more flaming in nature. The CHOCHO to CO NEMRs did

DOI: 10.1021/acs.est.7b03517
Environ. Sci. Technol. 2017, 51, 11761−11770

not appear to vary strongly with MCE, consistent with previous measurements of HCHO and CH_3COCHO emission ratios that were independent of MCE.[4] The CHOCHO to CO NEMRs as a function of MCE are shown in the supplement (Figure S3).

CHOCHO Emissions. NEMRs for CHOCHO with respect to CO and HCHO are shown in Figure 3 for all the plume intercepts. Additionally, ratios of CHOCHO to CO and HCHO from the literature are shown. The CHOCHO to CO NEMRs from the field averaged 0.0016 ± 0.0009, higher than the single CHOCHO to CO emission ratio from laboratory data,[20] but a factor of 4 lower than the value used by Fu et al. for the global CHOCHO budget,[22] which used emission ratios derived from the two earlier laboratory studies.[20,21] The field CHOCHO to HCHO NEMRs range from 0.008 to 0.11, with an average of 0.038 ± 0.02. The CHOCHO to HCHO ratios observed here are consistent with those observed several hours downwind of a fire in California[14] and with satellite observations over Africa during the burning season,[13] but are significantly lower than previous laboratory measurements, which average 1.18 (i.e., a greater than 1:1 molar ratio of CHOCHO to HCHO emission). The literature values closest to the field data are from burning a synthetic log and mixed hardwoods in a wood stove, combustion sources unlikely to be representative of what was observed from the aircraft.

Since the plumes potentially were aged, we will consider processes that could cause the observed NEMRs to be lower than the literature emission ratios. The lower NEMRs could be due to a preferential production of HCHO or a preferential loss of CHOCHO due to OH oxidation, photolysis, or aerosol uptake. For the night intercepts, aerosol uptake should be the main process affecting CHOCHO NEMRs. Photolysis does not occur at night, and since a large source of OH in fire plumes is the photolysis of HONO and HCHO,[6,45,47,48] OH concentrations are expected to be much lower in the nighttime plumes. Liu et al. observed little to no O_3 and PAN production in a fire plume intercepted near sunset, in contrast to faster production of those species in daytime plumes,[5] supporting limited photochemistry in these fire plumes at night. For these reasons, we will first discuss the nighttime intercepts from SENEX.

HCHO has a low Henry's law coefficient[49] and is not known to be taken up by aerosol,[50] but CHOCHO has a Henry's coefficient 2 to 4 orders of magnitude higher[51] and is readily taken up by wet aerosol.[50,52−54] Past work has shown that aerosol liquid water content plays a major role in controlling the amount of CHOCHO taken up by aerosol.[53,55] However, biomass burning particles are known to be less hygroscopic than other aerosol particle types.[3,45,56,57] Only a few measurements of particle water uptake were available in the fire plumes, but little to no optical growth due to humidification was observed in those measurements, consistent with the aerosol being less hygroscopic. Even though the relative humidity during the nighttime intercepts was high (>80%), the limited growth observed during SENEX, in addition to previous work, suggest that there was little water present in the aerosol in the biomass burning plumes, limiting the amount of CHOCHO uptake.

Determining the magnitude of potential aerosol uptake is complicated since the fire locations, and thus their transport distance and time to the aircraft, are not known. However, eight of the ten intercepts performed on the night of 2/3 July 2013 were potentially from the same fire based on location and wind direction. The fire location was unknown, but it was likely northwest of the town of New Madrid, MO, consistent with wind direction and the locations of fires before and after the date of the flight. These plumes were sampled over several hours in many locations, so any changes in the NEMRs could simply be due to sampling smoke from different stages of the fire. Dilution into air masses with different background concentrations of the species of interest could also affect the NEMR,[58] but we do not expect this to be an issue at night. The plume intercepted at 21:46 CDT is downwind of the plume intercepted at 20:55 CDT (outlined in black in Figure 1b), and based on wind speed, the time between the intercepts (48 min) was close to the transport time (~40 min) between these two locations. The intercept altitudes were within 50 m of each other, and the variation in the background levels of CO, HCHO, and CHOCHO were small compared to the enhancements of those species, so it is unlikely that there was mixing into air with different backgrounds that could have affected the NEMR.[58]

The CHOCHO to CO NEMR was larger in the downwind intercept (0.0014 compared to 0.0010), as was the CHOCHO to HCHO NEMR (0.037 to 0.031). These increases are smaller than the uncertainties, so it is not possible to assess potential CHOCHO production through dark reactions. However, the aerosol surface area (>3000 $\mu m^2/m^3$) and the RH (>90%) were high in both intercepts, so assuming that nighttime production was negligible, if there had been rapid aerosol uptake of CHOCHO we should have observed clear evidence for a decrease in CHOCHO during plume transport.

Due to changes in the wind direction during the course of the flight, we cannot discern which of the other six intercepts, if any, were downwind of others. Since we do not know the exact location of the fires, we cannot calculate an exact distance from the source. However, since it is likely that New Madrid, MO was between the fire and the WP-3D aircraft, we can estimate the distance from the source using New Madrid as a reference point. The CHOCHO to CO and HCHO NEMRs as a function of distance from New Madrid are shown in Figure 4. The background levels of all relevant species were constant for all eight intercepts, and the intercept altitudes were generally within 200 m of each other. In general, the greater the distance from the source to the plume, the higher the CHOCHO to CO NEMR, which we would not expect if aerosol uptake were the most important process affecting CHOCHO to CO NEMRs. The CHOCHO to HCHO NEMRs also increased, but that trend was not as apparent.

For the daytime intercepts, both photochemistry and aerosol uptake could affect the CHOCHO NEMRs. We do not have a way to determine the age of plumes intercepted during the day during SENEX. However, the age of the two plumes intercepted during SONGNEX can be estimated with reasonable certainty. Two fires were identified in the FINN database near the intercept in Florida on 19 March 2015, both roughly 8.5 km upwind. Using the windspeed measured on the plane at the time of the intercept, the transport time from either fire was approximately 45 min. For the plume intercepted in Oklahoma on 20 April 2015, no fire was found in the FINN database. However, the plume was intercepted at 15:53 CDT on a relatively warm and sunny day, and over 0.4 ppbv of HONO was measured, with a HONO to CO NEMR of 0.002. Several studies have found that the HONO to CO ratio decreases downwind of daytime fires, sometimes by as a much as a factor of 10 over 20 min,[37,45] implying that the loss of

DOI: 10.1021/acs.est.7b03517
Environ. Sci. Technol. 2017, 51, 11761−11770

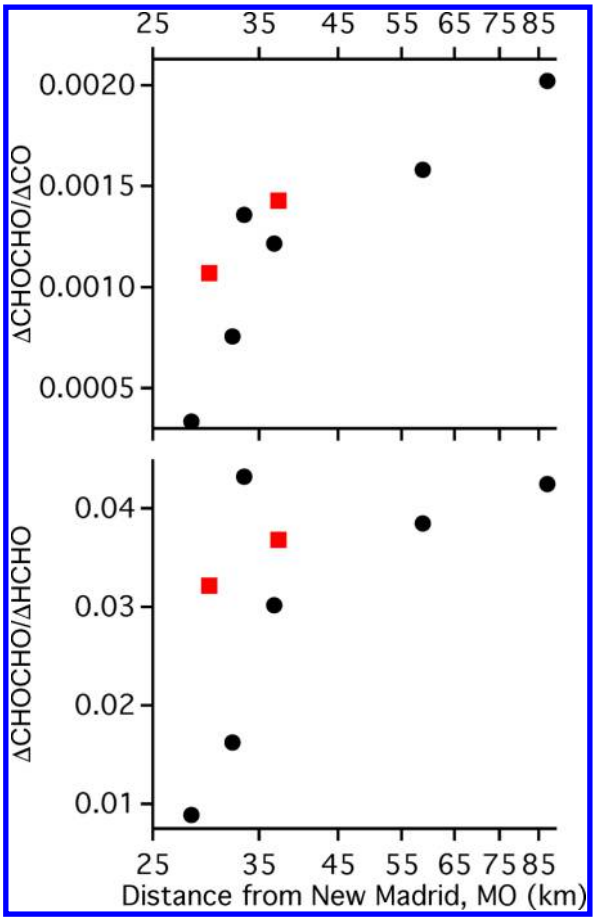

Figure 4. CHOCHO NEMRs relative to CO and HCHO as a function of distance from the town of New Madrid, MO. The intercept at 21:46 is downwind of the intercept at 20:55 (both marked with red squares).

HONO far outweighs production in daytime fire plumes. If we assume that the only loss of HONO is due to photolysis, and that the production rate is sufficiently small compared to the loss rate that it can be ignored, we can estimate the plume age using the measured HONO NEMR, an estimate for the initial emission ratio, and the calculated photolysis rate. Stockwell et al. report an average HONO emission ratio of 0.0045 for all fuel types.[4] Taking this as the initial value and using photolysis rates from the National Center for Atmospheric Research Tropospheric Ultraviolet and Visible (NCAR TUV) model[59,60] gives a plume age of roughly 9 min.

Particle composition and water uptake were not measured during SONGNEX, but we expect that the particles will take up little water, similar to what was observed during SENEX. Additionally, the relative humidity during the SONGNEX intercepts was much lower than observed for the SENEX intercepts. In Florida the humidity was 62%, below the deliquescence relative humidity for laboratory generated biomass burning aerosol,[61,62] while the humidity in Oklahoma was only 34%, at or below the efflorescence relative humidity of many common atmospheric salts,[63] so the aerosol should have been dry or nearly so. In chamber experiments with dry aerosol seed, no CHOCHO uptake was observed,[50,52] so it is likely that CHOCHO loss to aerosol was even more limited for the SONGNEX intercepts than during SENEX.

Since these two intercepts happened during the day, photolysis and oxidation by OH will reduce the observed CHOCHO concentrations and NEMRs. Using the plume ages calculated earlier, we can estimate the magnitude of this effect for the SONGNEX data from the photolysis rates from the TUV model. No OH measurements were available, so a value of 1×10^7 molecules cm^{-3} was used for both plumes,[45] although values half as large have been observed in fires.[56] The OH concentration used is likely higher than the actual values, so the CHOCHO losses calculated here are upper limits. For the Florida plume, this gives an estimated loss of 45%. However, a loss of 71% is required to bring the observed NEMR into agreement with the value from Fu et al.[22] For Oklahoma the calculated loss is only 11%, but the observed NEMR is 30% lower than the model CHOCHO emission rate. If we include aerosol uptake using a high value of $\gamma = 2 \times 10^{-3}$ for the uptake coefficient,[46] the CHOCHO loss is 15%, still too low to close the gap between the literature emission ratio and

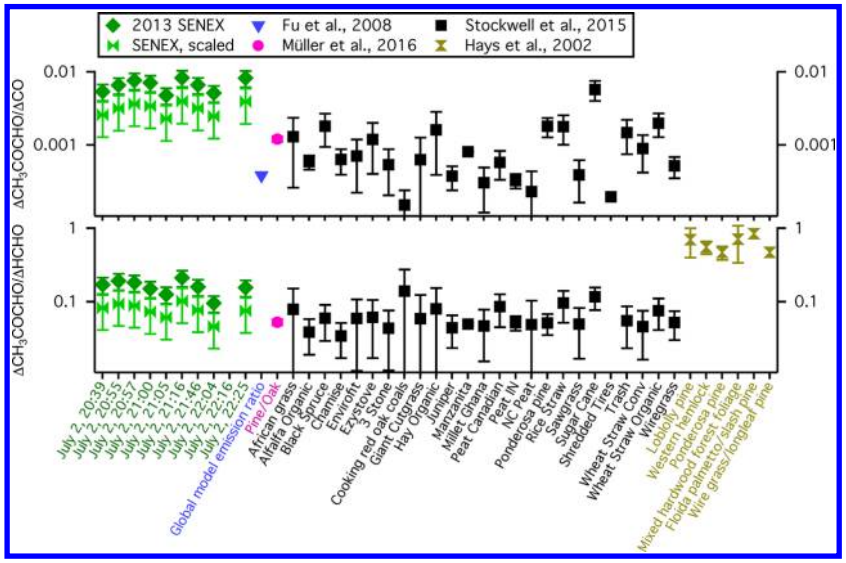

Figure 5. NEMRs from the nighttime intercepts during the 2013 SENEX campaign and literature emission ratios for CH_3COCHO against CO (top) and HCHO (bottom). Scaled values are corrected for the interference from biacetyl ($CH_3COCOCH_3$). No CH_3COCHO was observed during daytime intercepts during either SENEX or SONGNEX.

DOI: 10.1021/acs.est.7b03517
Environ. Sci. Technol. 2017, 51, 11761−11770

the measured NEMR. Particle concentration measurements were not available for the Florida intercept, but given the hydrophobic nature of biomass burning aerosol, it is likely that aerosol uptake of CHOCHO was also limited during that time.

The same photochemical processes that reduce the CHOCHO to CO NEMRs during the day could also reduce the CHOCHO to HCHO NEMRs. However, CHOCHO and HCHO have similar photolysis rate constants[28,64] and similar rate constants with respect to OH,[65,66] so their loss rates will be similar. Numerous studies have observed increases in HCHO downwind of daytime fires due to oxidation of various precursors by OH.[25,45,47,56] These increases range from a factor of 1.5 over 4 h[56] to a factor of 3.7 in 0.5 h.[47] The observed increases in HCHO are still insufficient to explain the nearly factor of 10 discrepancy between the Florida and Oklahoma CHOCHO to HCHO NEMRs and the literature values. Additionally, many of the VOCs that produce HCHO can also produce CHOCHO, with the ratio of the CHOCHO yield to the HCHO yield ranging from ~0.03 for species like ethene to over 10 for acetylene,[19] so any increases in HCHO downwind of fires may be partially offset by increases in CHOCHO. Fully examining the evolution of carbonyl compounds downwind of fires is beyond the scope of this paper, but should be investigated in future laboratory and field work.

CH_3COCHO Emissions. CH_3COCHO NEMRs against CO and HCHO from the SENEX nighttime intercepts are shown in Figure 5, as are ratios from previous studies. CH_3COCHO was not observed during any of the daytime intercepts. The mixing ratios of CHOCHO in the daytime plumes generally were low (~200−300 pptv), and based on the night intercepts, CH_3COCHO is emitted at two to four times the rate of CHOCHO. Assuming a similar ratio for the daytime plumes, even without including loss processes the CH_3COCHO concentrations would have been below the ACES detection limit for CH_3COCHO of several ppbv.

Our CH_3COCHO to CO NEMRs average 0.006 ± 0.001, a factor of 6 higher than reported previously.[4,25] The CH_3COCHO to HCHO NEMRs are in better agreement with those studies, but our HCHO to CO NEMRs are two to three times higher than those from past work, and the increased HCHO brings the observed CH_3COCHO to HCHO NEMRs closer to the literature values for the CH_3COCHO to HCHO emission ratios. These two studies both measured CH_3COCHO using PTR-MS, and in experiments where CH_3COCHO was injected into an environmental chamber, a PTR-MS instrument and broadband absorption instruments similar to the one used here agreed within 25%.[16] While these techniques may agree when only CH_3COCHO is present, in fire plumes there are other species that potentially have similar absorption cross sections or the same mass as CH_3COCHO, which could interfere with both techniques.

Substituted bicarbonyls such as biacetyl ($CH_3COCOCH_3$) are emitted from fires in large quantities and have visible absorption cross sections similar to that of CH_3COCHO. Thalman et al. did not observe an interference when both CH_3COCHO and biacetyl were present,[16] but the biacetyl concentrations were a factor of 3 lower than the CH_3COCHO concentrations in those experiments,[16] while the reverse will be true in fires.[4] Also, the instrument used by Thalman et al. was operated at a higher resolution (0.5 nm) than our instrument (1 nm), and at the lower resolution used by ACES we will not be able to robustly retrieve CH_3COCHO and biacetyl concentrations. Species with the same mass as CH_3COCHO such as propenoic acid (CH_2 = CHCOOH) have been reported in fire emissions analyzed using GC-MS,[67] but since CH_3COCHO was not reported the fraction of the signal from each species is not known.

We attempted to correct the retrieved CH_3COCHO concentrations using the literature cross sections for CH_3COCHO,[68] biacetyl,[69] and acetylpropionyl ($CH_3COCOCH_2H_3$)[70] (all shown in Figure S4) and previously reported emission rates,[4] assuming that the observed signal attributed to CH_3COCHO is actually the sum of the emissions of all three bicarbonyls weighted by their absorption cross sections.

$$N_{\text{methylglyoxal,cor}} = \frac{N_{\text{methylglyoxal,apparent}}}{1 + E_{\text{biacetyl}}C_{\text{biacetyl}} + E_{\text{acetylpropionyl}}C_{\text{acetylpropionyl}}} \quad (3)$$

where E_X is the emission ratio of the given bicarbonyl divided by the emission ratio for CH_3COCHO, and C_X is the cross section for the bicarbonyl divided by the CH_3COCHO cross section. The emission ratios in Stockwell et al. are reported for given masses,[4] and we assumed that all the signal at a given mass was from the corresponding bicarbonyl. We used the average emission ratio for each mass over all the fuel types, and since the cross section ratios are not constant, both the cross section ratios at 445 and 450 nm were used. This gives a correction factor of 2 ± 0.5, and results in an average CH_3COCHO to CO NEMR of 0.003 ± 0.001, still roughly three times greater than previously reported ("scaled" points shown in Figure 5). Whether this is due to coemitted species with the same mass or with similar absorption cross sections is not known, and further work is needed to resolve this discrepancy.

Implications. The impact of applying the lower CHOCHO NEMRs to global emissions from biomass burning will depend on how the emissions vary with fuel type. Stockwell et al. examined several crop types such as rice straw and wheat and found the HCHO emissions from those fuels to be close to or greater than the median HCHO emission ratio.[4] Additionally, Akagi et al. found burning crop residue to be the third highest emitter of HCHO.[3] It is likely that the fire plumes examined here were from agricultural fires. If we assume that, like HCHO, CHOCHO emission ratios from burning crops are generally higher than from other fuels, then CHOCHO emission ratios from other fuels are likely to be the same or lower than the values reported here for agricultural fires, which are already a factor of 2−4 lower than the value used in the global budget.[22] Measurements of CHOCHO emissions from other fuel types are needed, but if the trend for HCHO holds for CHOCHO, then CHOCHO emissions from all fuel types are likely overestimated.

Modeling results indicate that primary CHOCHO emissions from biomass burning contribute 12% of the global CHOCHO budget.[22] If the CHOCHO emission ratios from other fires are similar to the fires examined here, the contribution of biomass burning to the global CHOCHO budget may be overestimated by up to a factor of 4, reducing the CHOCHO emissions from 5.2 Tg a^{-1} to only 1.3 Tg a^{-1}, and much smaller than the source from isoprene oxidation of 21 Tg a^{-1}. CHOCHO emissions from fires are likely to be variable, and CHOCHO could be formed in plumes downwind of fires by processes that require

DOI: 10.1021/acs.est.7b03517
Environ. Sci. Technol. 2017, 51, 11761−11770

further study to accurately quantify. The CHOCHO to HCHO NEMRs observed here are consistent with the ratios retrieved by satellites over areas dominated by biomass burning (~0.08),[13] but are several times higher than ambient CHOCHO to HCHO ratios in nonbiomass burning influenced regions (~0.02−0.04).[14,15] However, there is considerable uncertainty in the downwind ratio of CHOCHO to HCHO since yields of these species from common biomass burning VOCs need to be measured more accurately. Laboratory experiments on biomass burning emissions, combined with field measurements such as these in larger fire plumes, will aid in the use of CHOCHO as a tracer for biomass burning emissions from satellites and will help improve global budgets of carbonyl emissions.

■ ASSOCIATED CONTENT

Supporting Information

The Supporting Information is available free of charge on the ACS Publications website at DOI: 10.1021/acs.est.7b03517.

Example fits; NEMRs and literature emission ratios for other species; CHOCHO NEMRs as a function of MCE; absorption cross sections for several substituted bicarbonyls; tables with details on the plume intercepts, including retrieved CHOCHO NEMRs (PDF)

■ AUTHOR INFORMATION

Corresponding Author

*S. S. Brown. Email: steven.s.brown@noaa.gov, Phone: 303 497 6306, Fax: 303 497 5126.

ORCID

Kyle J. Zarzana: 0000-0003-1581-6419

John B. Nowak: 0000-0002-5697-9807

Present Addresses

[#]School of Earth Science & Environmental Engineering, Gwangju Institute of Science & Technology, Gwangju 61005, Korea

[⊗]School of Engineering & Applied Sciences, Harvard University, Cambridge, MA 02138, USA

[Δ]Chemistry and Dynamics Branch, NASA Langley Research Center, Hampton, VA 23681, USA

[∇]School of Engineering & Applied Sciences & Department of Chemistry & Chemical Biology, Harvard University, Cambridge, MA 02138, USA

Notes

The authors declare no competing financial interest.

■ ACKNOWLEDGMENTS

The authors thank all those who participated in the SENEX and SONGNEX campaigns, particularly the pilots and support crews from the NOAA Aircraft Operations Center. We thank J. S. Holloway for the CO and SO_2 data, C. A. Brock for the aerosol number concentration data, and J. P. Schwarz and M. Z. Markovic for the black carbon data. K.-E. Min acknowledges a postdoctoral fellowship from the Cooperative Institute for Research in Environmental Sciences at the University of Colorado. J. Kaiser acknowledges support from NASA Headquarters under the NASA Earth and Space Science Fellowship Program grant NNX14AK97H. The HCHO measurements were supported by US EPA Science to Achieve Results (STAR) program grant 83540601 and NASA-GeoCAPE award number NNX15AH83G.

■ REFERENCES

(1) Crutzen, P. J.; Andreae, M. O. Biomass burning in the tropics: Impact on atmospheric chemistry and biogeochemical cycles. *Science* **1990**, *250*, 1669−1678.

(2) Brey, S. J.; Fischer, E. V. Smoke in the city: How often and where does smoke impact summertime ozone in the United States? *Environ. Sci. Technol.* **2016**, *50*, 1288−1294.

(3) Akagi, S. K.; Yokelson, R. J.; Wiedinmyer, C.; Alvarado, M. J.; Reid, J. S.; Karl, T.; Crounse, J. D.; Wennberg, P. O. Emission factors for open and domestic biomass burning for use in atmospheric models. *Atmos. Chem. Phys.* **2011**, *11*, 4039−4072.

(4) Stockwell, C. E.; Veres, P. R.; Williams, J.; Yokelson, R. J. Characterization of biomass burning emissions from cooking fires, peat, crop residue, and other fuels with high-resolution proton-transfer-reaction time-of-flight mass spectrometry. *Atmos. Chem. Phys.* **2015**, *15*, 845−865.

(5) Liu, X.; Zhang, Y.; Huey, L. G.; Yokelson, R. J.; Wang, Y.; Jimenez, J. L.; Campuzano-Jost, P.; Beyersdorf, A. J.; Blake, D. R.; Choi, Y. St.; St. Clair, J. M.; Crounse, J. D.; Day, D. A.; Diskin, G. S.; Fried, A.; Hall, S. R.; Hanisco, T. F.; King, L. E.; Meinardi, S.; Mikoviny, T.; Palm, B. B.; Peischl, J.; Perring, A. E.; Pollack, I. B.; Ryerson, T. B.; Sachse, G.; Schwarz, J. P.; Simpson, I. J.; Tanner, D. J.; Thornhill, K. L.; Ullmann, K.; Weber, R. J.; Wennberg, P. O.; Wisthaler, A.; Wolfe, G. M.; Ziemba, L. D. Agricultural fires in the southeastern U.S. during SEAC[4]RS: Emissions of trace gases and particles and evolution of ozone, reactive nitrogen, and organic aerosol. *J. Geophys. Res.* **2016**, *121*, 7383−7414.

(6) Mason, S. A.; Field, R. J.; Yokelson, R. J.; Kochivar, M. A.; Tinsley, M. R.; Ward, D. E.; Hao, W. M. Complex effects arising in smoke plume simulations due to inclusion of direct emissions of oxygenated organic species from biomass combustion. *J. Geophys. Res.* **2001**, *106*, 12527−12539.

(7) Volkamer, R.; Sheehy, P.; Molina, L. T.; Molina, M. J. Oxidative capacity of the Mexico City atmosphere − Part 1: A radical source perspective. *Atmos. Chem. Phys.* **2010**, *10*, 6969−6991.

(8) Edwards, P. M.; Brown, S. S.; Roberts, J. M.; Ahmadov, R.; Banta, R. M.; deGouw, J. A.; Dube, W. P.; Field, R. A.; Flynn, J. H.; Gilman, J. B.; Graus, M.; Helmig, D.; Koss, A.; Langford, A. O.; Lefer, B. L.; Lerner, B. M.; Li, R.; Li, S.-M.; McKeen, S. A.; Murphy, S. M.; Parrish, D. D.; Senff, C. J.; Soltis, J.; Stutz, J.; Sweeney, C.; Thompson, C. R.; Trainer, M. K.; Tsai, C.; Veres, P. R.; Washenfelder, R. A.; Warneke, C.; Wild, R. J.; Young, C. J.; Yuan, B.; Zamora, R. High winter ozone pollution from carbonyl photolysis in an oil and gas basin. *Nature* **2014**, *514*, 351−354.

(9) Volkamer, R.; San Martini, F.; Molina, L. T.; Salcedo, D.; Jimenez, J. L.; Molina, M. J. A missing sink for gas-phase glyoxal in Mexico City: Formation of secondary organic aerosol. *Geophys. Res. Lett.* **2007**, *34*, L19807.

(10) De Haan, D. O.; Tolbert, M. A.; Jimenez, J. L. Atmospheric condensed-phase reactions of glyoxal with methylamine. *Geophys. Res. Lett.* **2009**, *36*, L11819.

(11) Shapiro, E. L.; Szprengiel, J.; Sareen, N.; Jen, C. N.; Giordano, M. R.; McNeill, V. F. Light-absorbing secondary organic material formed by glyoxal in aqueous aerosol mimics. *Atmos. Chem. Phys.* **2009**, *9*, 2289−2300.

(12) Wittrock, F.; Richter, A.; Oetjen, H.; Burrows, J. P.; Kanakidou, M.; Myriokefalitakis, S.; Volkamer, R.; Beirle, S.; Platt, U.; Wagner, T. Simultaneous global observations of glyoxal and formaldehyde from space. *Geophys. Res. Lett.* **2006**, *33*, L16804.

(13) Chan Miller, C.; Gonzalez Abad, G.; Wang, H.; Liu, X.; Kurosu, T.; Jacob, D. J.; Chance, K. Glyoxal retrieval from the Ozone Monitoring Instrument. *Atmos. Meas. Tech.* **2014**, *7*, 3891−3907.

(14) DiGangi, J. P.; Henry, S. B.; Kammrath, A.; Boyle, E. S.; Kaser, L.; Schnitzhofer, R.; Graus, M.; Turnipseed, A.; Park, J.-H.; Weber, R. J.; Hornbrook, R. S.; Cantrell, C. A.; Maudlin, R. L., III; Kim, S.; Nakashima, Y.; Wolfe, G. M.; Kajii, Y.; Apel, E. C.; Goldstein, A. H.; Guenther, A.; Karl, T.; Hansel, A.; Keutsch, F. N. Observations of glyoxal and formaldehyde as metrics for the anthropogenic impact on rural photochemistry. *Atmos. Chem. Phys.* **2012**, *12*, 9529−9543.

(15) Kaiser, J.; Wolfe, G. M.; Min, K. E.; Brown, S. S.; Miller, C. C.; Jacob, D. J.; deGouw, J. A.; Graus, M.; Hanisco, T. F.; Holloway, J.; Peischl, J.; Pollack, I. B.; Ryerson, T. B.; Warneke, C.; Washenfelder, R. A.; Keutsch, F. N. Reassessing the ratio of glyoxal to formaldehyde as an indicator of hydrocarbon precursor speciation. *Atmos. Chem. Phys.* **2015**, *15*, 7571−7583.
(16) Thalman, R.; Baeza-Romero, M. T.; Ball, S. M.; Borrás, E.; Daniels, M. J. S.; Goodall, I. C. A.; Henry, S. B.; Karl, T.; Keutsch, F. N.; Kim, S.; Mak, J.; Monks, P. S.; Muñoz, A.; Orlando, J.; Peppe, S.; Rickard, A. R.; Ródenas, M.; Sánchez, P.; Seco, R.; Su, L.; Tyndall, G.; Vázquez, M.; Vera, T.; Waxman, E.; Volkamer, R. Instrument intercomparison of glyoxal, methyl glyoxal and NO_2 under simulated atmospheric conditions. *Atmos. Meas. Tech.* **2015**, *8*, 1835−1862.
(17) Min, K.-E.; Washenfelder, R. A.; Dubé, W. P.; Langford, A. O.; Edwards, P. M.; Zarzana, K. J.; Stutz, J.; Lu, K.; Rohrer, F.; Zhang, Y.; Brown, S. S. A broadband cavity enhanced absorption spectrometer for aircraft measurements of glyoxal, methylglyoxal, nitrous acid, nitrogen dioxide, and water vapor. *Atmos. Meas. Tech.* **2016**, *9*, 423−440.
(18) Volkamer, R.; Molina, L. T.; Molina, M. J.; Shirley, T.; Brune, W. H. DOAS measurement of glyoxal as an indicator for fast VOC chemistry in urban air. *Geophys. Res. Lett.* **2005**, *32*, L08806.
(19) Chan Miller, C.; Jacob, D. J.; González Abad, G.; Chance, K. Hotspot of glyoxal over the Pearl River delta seen from the OMI satellite instrument: implications for emissions of aromatic hydrocarbons. *Atmos. Chem. Phys.* **2016**, *16*, 4631−4639.
(20) McDonald, J. D.; Zielinska, B.; Fujita, E. M.; Sagebiel, J. C.; Chow, J. C.; Watson, J. G. Fine particle and gaseous emission rates from residential wood combustion. *Environ. Sci. Technol.* **2000**, *34*, 2080−2091.
(21) Hays, M. D.; Geron, C. D.; Linna, K. J.; Smith, N. D.; Schauer, J. J. Speciation of gas-phase and fine particle emissions from burning of foliar fuels. *Environ. Sci. Technol.* **2002**, *36*, 2281−2295.
(22) Fu, T.-M.; Jacob, D. J.; Wittrock, F.; Burrows, J. P.; Vrekoussis, M.; Henze, D. K. Global budgets of atmospheric glyoxal and methylglyoxal, and implications for formation of secondary organic aerosols. *J. Geophys. Res.* **2008**, *113*, D15303.
(23) Karst, U.; Binding, N.; Cammann, K.; Witting, U. Interferences of nitrogen dioxide in the determination of aldehydes and ketones by sampling on 2,4-dinitrophenylhydrazine-coated solid sorbent. *Fresenius' J. Anal. Chem.* **1993**, *345*, 48−52.
(24) Achatz, S.; Lörinci, G.; Hertkorn, N.; Gebefügi, I.; Kettrup, A. Disturbance of the determination of aldehydes and ketones: Structural elucidation of degradation products derived from the reaction of 2,4-dinitrophenylhydrazine (DNPH) with ozone. *Fresenius' J. Anal. Chem.* **1999**, *364*, 141−146.
(25) Müller, M.; Anderson, B. E.; Beyersdorf, A. J.; Crawford, J. H.; Diskin, G. S.; Eichler, P.; Fried, A.; Keutsch, F. N.; Mikoviny, T.; Thornhill, K. L.; Walega, J. G.; Weinheimer, A. J.; Yang, M.; Yokelson, R. J.; Wisthaler, A. situ measurements and modeling of reactive trace gases in a small biomass burning plume. *Atmos. Chem. Phys.* **2016**, *16*, 3813−3824.
(26) Stönner, C.; Derstroff, B.; Klüpfel, T.; Crowley, J. N.; Williams, J. Glyoxal measurement with a proton transfer reaction time of flight mass spectrometer (PTR-TOF-MS): characterization and calibration. *J. Mass Spectrom.* **2017**, *52*, 30−35.
(27) Huisman, A. J.; Hottle, J. R.; Coens, K. L.; DiGangi, J. P.; Galloway, M. M.; Kammrath, A.; Keutsch, F. N. Laser-induced phosphorescence for the in situ detection of glyoxal at part per trillion mixing ratios. *Anal. Chem.* **2008**, *80*, 5884−5891.
(28) Volkamer, R.; Spietz, P.; Burrows, J.; Platt, U. High-resolution absorption cross-section of glyoxal in the UV-vis and IR spectral ranges. *J. Photochem. Photobiol., A* **2005**, *172*, 35−46.
(29) Washenfelder, R. A.; Langford, A. O.; Fuchs, H.; Brown, S. S. Measurement of glyoxal using an incoherent broadband cavity enhanced absorption spectrometer. *Atmos. Chem. Phys.* **2008**, *8*, 7779−7793.
(30) Thalman, R.; Volkamer, R. Inherent calibration of a blue LED-CE-DOAS instrument to measure iodine oxide, glyoxal, methyl glyoxal, nitrogen dioxide, water vapour and aerosol extinction in open cavity mode. *Atmos. Meas. Tech.* **2010**, *3*, 1797−1814.
(31) Warneke, C.; Trainer, M.; de Gouw, J. A.; Parrish, D. D.; Fahey, D. W.; Ravishankara, A. R.; Middlebrook, A. M.; Brock, C. A.; Roberts, J. M.; Brown, S. S.; Neuman, J. A.; Lerner, B. M.; Lack, D.; Law, D.; Hübler, G.; Pollack, I.; Sjostedt, S.; Ryerson, T. B.; Gilman, J. B.; Liao, J.; Holloway, J.; Peischl, J.; Nowak, J. B.; Aikin, K. C.; Min, K.-E.; Washenfelder, R. A.; Graus, M. G.; Richardson, M.; Markovic, M. Z.; Wagner, N. L.; Welti, A.; Veres, P. R.; Edwards, P.; Schwarz, J. P.; Gordon, T.; Dube, W. P.; McKeen, S. A.; Brioude, J.; Ahmadov, R.; Bougiatioti, A.; Lin, J. J.; Nenes, A.; Wolfe, G. M.; Hanisco, T. F.; Lee, B. H.; Lopez-Hilfiker, F. D.; Thornton, J. A.; Keutsch, F. N.; Kaiser, J.; Mao, J.; Hatch, C. D. Instrumentation and measurement strategy for the NOAA SENEX aircraft campaign as part of the Southeast Atmosphere Study 2013. *Atmos. Meas. Tech.* **2016**, *9*, 3063−3093.
(32) Platt, U.; Stutz, J. *Differential Optical Absorption Spectroscopy: Principles and Applications*; Springer: Berlin, 2008; 10.1007/978-3-540-75776-4.
(33) Kraus, S. G. *DOASIS: A Framework Design for DOAS*. Ph.D. thesis, University of Mannheim, Mannheim, Germany, 2006.
(34) Holloway, J. S.; Jakoubek, R. O.; Parrish, D. D.; Gerbig, C.; Volz-Thomas, A.; Schmitgen, S.; Fried, A.; Wert, B.; Henry, B.; Drummond, J. R. Airborne intercomparison of vacuum ultraviolet fluorescence and tunable diode laser absorption measurements of tropospheric carbon monoxide. *J. Geophys. Res.* **2000**, *105*, 24251−24261.
(35) Cazorla, M.; Wolfe, G. M.; Bailey, S. A.; Swanson, A. K.; Arkinson, H. L.; Hanisco, T. F. A new airborne laser-induced fluorescence instrument for in situ detection of formaldehyde throughout the troposphere and lower stratosphere. *Atmos. Meas. Tech.* **2015**, *8*, 541−552.
(36) Peischl, J.; Ryerson, T. B.; Holloway, J. S.; Trainer, M.; Andrews, A. E.; Atlas, E. L.; Blake, D. R.; Daube, B. C.; Dlugokencky, E. J.; Fischer, M. L.; Goldstein, A. H.; Guha, A.; Karl, T.; Kofler, J.; Kosciuch, E.; Misztal, P. K.; Perring, A. E.; Pollack, I. B.; Santoni, G. W.; Schwarz, J. P.; Spackman, J. R.; Wofsy, S. C.; Parrish, D. D. Airborne observations of methane emissions from rice cultivation in the Sacramento Valley of California. *J. Geophys. Res.* **2012**, *117*, D00V25.
(37) Neuman, J. A.; Trainer, M.; Brown, S. S.; Min, K.-E.; Nowak, J. B.; Parrish, D. D.; Peischl, J.; Pollack, I. B.; Roberts, J. M.; Ryerson, T. B.; Veres, P. R. HONO emission and production determined from airborne measurements over the Southeast U.S. *J. Geophys. Res.* **2016**, *121*, 9237−9250.
(38) Ryerson, T. B.; Buhr, M. P.; Frost, G. J.; Goldan, P. D.; Holloway, J. S.; Hübler, G.; Jobson, B. T.; Kuster, W. C.; McKeen, S. A.; Parrish, D. D.; Roberts, J. M.; Sueper, D. T.; Trainer, M.; Williams, J.; Fehsenfeld, F. C. Emissions lifetimes and ozone formation in power plant plumes. *J. Geophys. Res.* **1998**, *103*, 22569−22583.
(39) Brock, C. A.; Cozic, J.; Bahreini, R.; Froyd, K. D.; Middlebrook, A. M.; McComiskey, A.; Brioude, J.; Cooper, O. R.; Stohl, A.; Aikin, K. C.; de Gouw, J. A.; Fahey, D. W.; Ferrare, R. A.; Gao, R.-S.; Gore, W.; Holloway, J. S.; Hübler, G.; Jefferson, A.; Lack, D. A.; Lance, S.; Moore, R. H.; Murphy, D. M.; Nenes, A.; Novelli, P. C.; Nowak, J. B.; Ogren, J. A.; Peischl, J.; Pierce, R. B.; Pilewskie, P.; Quinn, P. K.; Ryerson, T. B.; Schmidt, K. S.; Schwarz, J. P.; Sodemann, H.; Spackman, J. R.; Stark, H.; Thomson, D. S.; Thornberry, T.; Veres, P.; Watts, L. A.; Warneke, C.; Wollny, A. G. Characteristics, sources, and transport of aerosols measured in spring 2008 during the aerosol, radiation, and cloud processes affecting Arctic Climate (ARCPAC) Project. *Atmos. Chem. Phys.* **2011**, *11*, 2423−2453.
(40) Langridge, J. M.; Richardson, M. S.; Lack, D.; Law, D.; Murphy, D. M. Aircraft instrument for comprehensive characterization of aerosol optical properties, part I: Wavelength-dependent optical extinction and its relative humidity dependence measured using cavity ringdown spectroscopy. *Aerosol Sci. Technol.* **2011**, *45*, 1305−1318.
(41) Schwarz, J. P.; Gao, R. S.; Fahey, D. W.; Thomson, D. S.; Watts, L. A.; Wilson, J. C.; Reeves, J. M.; Darbeheshti, M.; Baumgardner, D. G.; Kok, G. L.; Chung, S. H.; Schulz, M.; Hendricks, J.; Lauer, A.;

DOI: 10.1021/acs.est.7b03517
Environ. Sci. Technol. 2017, 51, 11761−11770

Kärcher, B.; Slowik, J. G.; Rosenlof, K. H.; Thompson, T. L.; Langford, A. O.; Loewenstein, M.; Aikin, K. C. Single-particle measurements of midlatitude black carbon and light-scattering aerosols from the boundary layer to the lower stratosphere. *J. Geophys. Res.* **2006**, *111*, D16207.
(42) Wiedinmyer, C.; Akagi, S. K.; Yokelson, R. J.; Emmons, L. K.; Al-Saadi, J. A.; Orlando, J. J.; Soja, A. J. The Fire INventory from NCAR (FINN): a high resolution global model to estimate the emissions from open burning. *Geosci. Model Dev.* **2011**, *4*, 625−641.
(43) US Department of Agriculture Forest Service, Active Fire Mapping Program. https://fsapps.nwcg.gov/afm/ (accessed 1 September 2017).
(44) US Department of Agriculture National Agricultural Statistics Service, CropScape-Cropland Data Layer. https://nassgeodata.gmu.edu/CropScape/ (accessed 23 May 2017).
(45) Yokelson, R. J.; Crounse, J. D.; DeCarlo, P. F.; Karl, T.; Urbanski, S.; Atlas, E.; Campos, T.; Shinozuka, Y.; Kapustin, V.; Clarke, A. D.; Weinheimer, A.; Knapp, D. J.; Montzka, D. D.; Holloway, J.; Weibring, P.; Flocke, F.; Zheng, W.; Toohey, D.; Wennberg, P. O.; Wiedinmyer, C.; Mauldin, L.; Fried, A.; Richter, D.; Walega, J.; Jimenez, J. L.; Adachi, K.; Buseck, P. R.; Hall, S. R.; Shetter, R. Emissions from biomass burning in the Yucatan. *Atmos. Chem. Phys.* **2009**, *9*, 5785−5812.
(46) Li, J.; Mao, J.; Min, K.-E.; Washenfelder, R. A.; Brown, S. S.; Kaiser, J.; Keutsch, F. N.; Volkamer, R.; Wolfe, G. M.; Hanisco, T. F.; Pollack, I. B.; Ryerson, T. B.; Graus, M.; Gilman, J. B.; Lerner, B. M.; Warneke, C.; de Gouw, J. A.; Middlebrook, A. M.; Liao, J.; Welti, A.; Henderson, B. H.; McNeill, V. F.; Hall, S. R.; Ullmann, K.; Donner, L. J.; Paulot, F.; Horowitz, L. W. Observational constraints on glyoxal production from isoprene oxidation and its contribution to organic aerosol over the Southeast United States. *J. Geophys. Res.* **2016**, *121*, 9849−9861.
(47) Akagi, S. K.; Yokelson, R. J.; Burling, I. R.; Meinardi, S.; Simpson, I.; Blake, D. R.; McMeeking, G. R.; Sullivan, A.; Lee, T.; Kreidenweis, S.; Urbanski, S.; Reardon, J.; Griffith, D. W. T.; Johnson, T. J.; Weise, D. R. Measurements of reactive trace gases and variable O_3 formation rates in some South Carolina biomass burning plumes. *Atmos. Chem. Phys.* **2013**, *13*, 1141−1165.
(48) Alvarado, M. J.; Lonsdale, C. R.; Yokelson, R. J.; Akagi, S. K.; Coe, H.; Craven, J. S.; Fischer, E. V.; McMeeking, G. R.; Seinfeld, J. H.; Soni, T.; Taylor, J. W.; Weise, D. R.; Wold, C. E. Investigating the links between ozone and organic aerosol chemistry in a biomass burning plume from a prescribed fire in California chaparral. *Atmos. Chem. Phys.* **2015**, *15*, 6667−6688.
(49) Sander, R. Compilation of Henry's law constants (version 4.0) for water as solvent. *Atmos. Chem. Phys.* **2015**, *15*, 4399−4981.
(50) Kroll, J. H.; Ng, N. L.; Murphy, S. M.; Varutbangkul, V.; Flagan, R. C.; Seinfeld, J. H. Chamber studies of secondary organic aerosol growth by reactive uptake of simple carbonyl compounds. *J. Geophys. Res.* **2005**, *110*, D23207.
(51) Waxman, E. M.; Elm, J.; Kurtén, T.; Mikkelsen, K. V.; Ziemann, P. J.; Volkamer, R. Glyoxal and methylglyoxal Setschenow salting constants in sulfate, nitrate, and chloride solutions: Measurements and Gibbs energies. *Environ. Sci. Technol.* **2015**, *49*, 11500−11508.
(52) Liggio, J.; Li, S.-M.; McLaren, R. Heterogeneous reactions of glyoxal on particulate matter: Identification of acetals and sulfate esters. *Environ. Sci. Technol.* **2005**, *39*, 1532−1541.
(53) Volkamer, R.; Ziemann, P. J.; Molina, M. J. Secondary Organic Aerosol Formation from Acetylene (C_2H_2): seed effect on SOA yields due to organic photochemistry in the aerosol aqueous phase. *Atmos. Chem. Phys.* **2009**, *9*, 1907−1928.
(54) Galloway, M. M.; Loza, C. L.; Chhabra, P. S.; Chan, A. W. H.; Yee, L. D.; Seinfeld, J. H.; Keutsch, F. N. Analysis of photochemical and dark glyoxal uptake: Implications for SOA formation. *Geophys. Res. Lett.* **2011**, *38*, L17811.
(55) Nakao, S.; Liu, Y.; Tang, P.; Chen, C.-L.; Zhang, J.; Cocker, D. R., III Chamber studies of SOA formation from aromatic hydrocarbons: observation of limited glyoxal uptake. *Atmos. Chem. Phys.* **2012**, *12*, 3927−3937.
(56) Akagi, S. K.; Craven, J. S.; Taylor, J. W.; McMeeking, G. R.; Yokelson, R. J.; Burling, I. R.; Urbanski, S. P.; Wold, C. E.; Seinfeld, J. H.; Coe, H.; Alvarado, M. J.; Weise, D. R. Evolution of trace gases and particles emitted by a chaparral fire in California. *Atmos. Chem. Phys.* **2012**, *12*, 1397−1421.
(57) Kreidenweis, S. M.; Asa-Awuku, A. In *Treatise on Geochemistry*, 2nd ed.; Turekian, H. D. H. K., Ed.; Elsevier: Oxford, 2014; Vol. 5, Chapter 5.13, pp 331−361, DOI: 10.1016/B978-0-08-095975-7.00418-6.
(58) Yokelson, R. J.; Andreae, M. O.; Akagi, S. K. Pitfalls with the use of enhancement ratios or normalized excess mixing ratios measured in plumes to characterize pollution sources and aging. *Atmos. Meas. Tech.* **2013**, *6*, 2155−2158.
(59) Madronich, S.; Flocke, S. In *Environmental Photochemistry*; Boule, P., Ed.; *The Handbook of Environmental Chemistry*; Springer-Verlag: Berlin, Heidelberg, 1999; pp 1−26, DOI: 10.1007/978-3-540-69044-3-1.
(60) NCAR/ACD, NCAR/ACD TUV: Tropospheric Ultraviolet and Visible Radiation Model. https://www2.acom.ucar.edu/modeling/tropospheric-ultraviolet-and-visible-tuv-radiation-model (accessed 5 June 2017).
(61) Day, D. E.; Hand, J. L.; Carrico, C. M.; Engling, G.; Malm, W. C. Humidification factors from laboratory studies of fresh smoke from biomass fuels. *J. Geophys. Res.* **2006**, *111*, D22202.
(62) Carrico, C. M.; Petters, M. D.; Kreidenweis, S. M.; Sullivan, A. P.; McMeeking, G. R.; Levin, E. J. T.; Engling, G.; Malm, W. C.; Collett, J. L., Jr. Water uptake and chemical composition of fresh aerosols generated in open burning of biomass. *Atmos. Chem. Phys.* **2010**, *10*, 5165−5178.
(63) Martin, S. T. Phase transitions of aqueous atmospheric particles. *Chem. Rev.* **2000**, *100*, 3403−3454.
(64) Röth, E.-P.; Ehhalt, D. H. A simple formulation of the CH_2O photolysis quantum yields. *Atmos. Chem. Phys.* **2015**, *15*, 7195−7202.
(65) Burkholder, J. B.; Sander, S. P.; Abbatt, J.; Barker, J. R.; Huie, R. E.; Kolb, C. E.; Kurylo, M. J.; Orkin, V. L.; Wilmouth, D. M.; Wine, P. H. *Chemical Kinetics and Photochemical Data for Use in Atmospheric Studies, Evaluation No. 18*; JPL Publication 15-10; Jet Propulsion Laboratory: Pasadena, CA, 2015; http://jpldataeval.jpl.nasa.gov.
(66) Feierabend, K. J.; Zhu, L.; Talukdar, R. K.; Burkholder, J. B. Rate coefficients for the OH + HC(O)C(O)H (glyoxal) reaction between 210 and 390 K. *J. Phys. Chem. A* **2008**, *112*, 73−82.
(67) Gilman, J. B.; Lerner, B. M.; Kuster, W. C.; Goldan, P. D.; Warneke, C.; Veres, P. R.; Roberts, J. M.; de Gouw, J. A.; Burling, I. R.; Yokelson, R. J. Biomass burning emissions and potential air quality impacts of volatile organic compounds and other trace gases from fuels common in the US. *Atmos. Chem. Phys.* **2015**, *15*, 13915−13938.
(68) Meller, R.; Raber, W.; Crowley, J.; Jenkin, M.; Moortgat, G. The UV-visible absorption spectrum of methylglyoxal. *J. Photochem. Photobiol., A* **1991**, *62*, 163−171.
(69) Horowitz, A.; Meller, R.; Moortgat, G. K. The UV-VIS absorption cross sections of the α-dicarbonyl compounds: pyruvic acid, biacetyl and glyoxal. *J. Photochem. Photobiol., A* **2001**, *146*, 19−27.
(70) Messaadia, L.; El Dib, G.; Ferhati, A.; Chakir, A. UV-visible spectra and gas-phase rate coefficients for the reaction of 2,3-pentanedione and 2,4-pentanedione with OH radicals. *Chem. Phys. Lett.* **2015**, *626*, 73−79.

DOI: 10.1021/acs.est.7b03517
Environ. Sci. Technol. 2017, 51, 11761−11770

Supporting information for:

Emissions of glyoxal and other carbonyl compounds from agricultural biomass burning plumes sampled by aircraft

Kyle J. Zarzana,[†,‡] Kyung-Eun Min,[†,‡,#] Rebecca A. Washenfelder,[†,‡] Jennifer Kaiser,[¶,@] Mitchell Krawiec-Thayer,[¶] Jeff Peischl,[†,‡] J. Andrew Neuman,[†,‡] John B. Nowak,[†,‡,△] Nicholas L. Wagner,[†,‡] William P. Dubè,[†,‡] Jason M. St. Clair,[§,‖] Glenn M. Wolfe,[§,‖] Thomas F. Hanisco,[§] Frank N. Keutsch,[¶,▽] Thomas B. Ryerson,[†] and Steven S. Brown[*,†,⊥]

†*NOAA Earth System Research Laboratory (ESRL) Chemical Sciences Division, Boulder, CO, USA*

‡*Cooperative Institute for Research in Environmental Sciences, University of Colorado Boulder, Boulder, CO, USA*

¶*Department of Chemistry, University of Wisconsin-Madison, Madison, WI, USA*

§*Atmospheric Chemistry & Dynamics Laboratory, NASA Goddard Space Flight Center, Greenbelt, MD, USA*

‖*Joint Center for Earth Systems Technology, University of Maryland Baltimore County, Baltimore, MD, USA*

⊥*Department of Chemistry & Biochemistry, University of Colorado Boulder, Boulder, CO, USA*

#*now at: School of Earth Science & Environmental Engineering, Gwangju Institute of Science & Technology, Gwangju, Korea*

@*now at: School of Engineering & Applied Sciences, Harvard University, Cambridge, MA, USA*

△*now at: Chemistry and Dynamics Branch, NASA Langley Research Center, Hampton, VA, USA*

▽*now at: School of Engineering & Applied Sciences & Department of Chemistry & Chemical Biology, Harvard University, Cambridge, MA, USA*

E-mail: steven.s.brown@noaa.gov

Phone: 303 497 6306. Fax: 303 497 5126

Supporting Information summary

Supporting Information pages: 9

Supporting Information figures: 4

Supporting Information tables: 3

Figures:

Figure S1: Sample fits for one plume intercept

Figure S2: NEMRs retrieved for CH_4, HCHO, and HONO

Figure S3: CHOCHO to CO NEMRs as a function of MCE

Figure S4: Substituted α-bicarbonyl absorption cross sections

Tables:

Table S1: Data on the SENEX nighttime intercepts

Table S2: Data on the SENEX daytime intercepts

Table S3: Data on the SONGNEX daytime intercepts

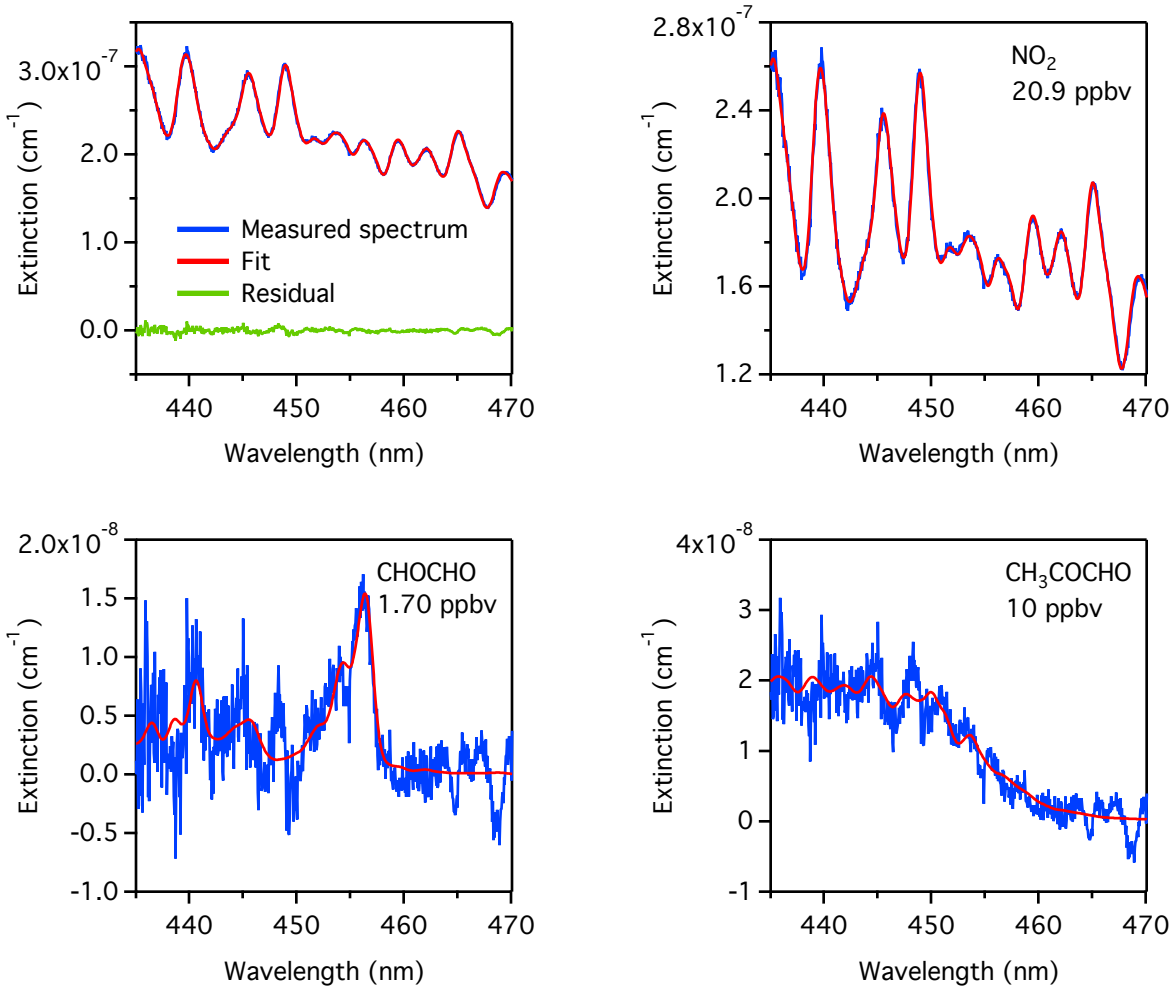

Figure S1: Sample fits for the plume intercepted at 20:55 CDT on 2 July 2013. Shown are the measured spectrum, total fit, and residuals (top left), as well as the fits for NO_2 (top right), CHOCHO (bottom left), and CH_3COCHO (bottom right)

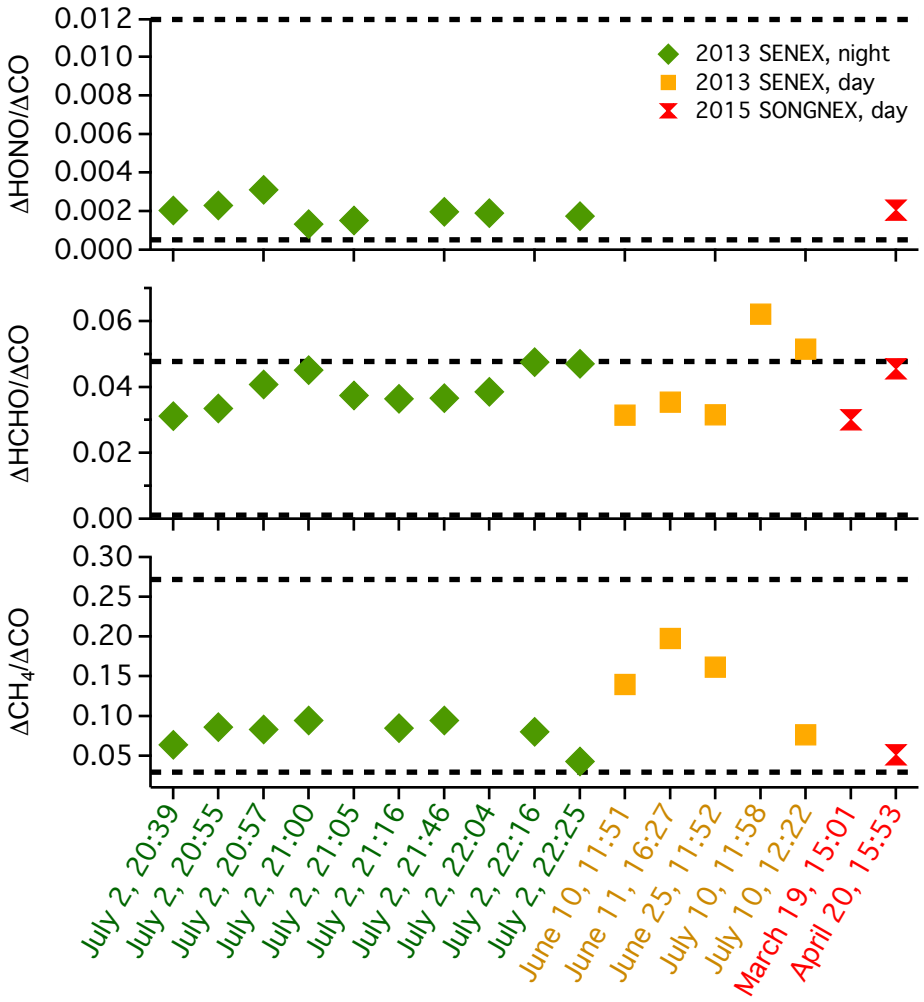

Figure S2: NEMRs for HONO, HCHO, and CH_4 retrieved in this study. The dashed lines denote the range of literature values for the emission ratio of the species from biomass burning.[S1–S4]

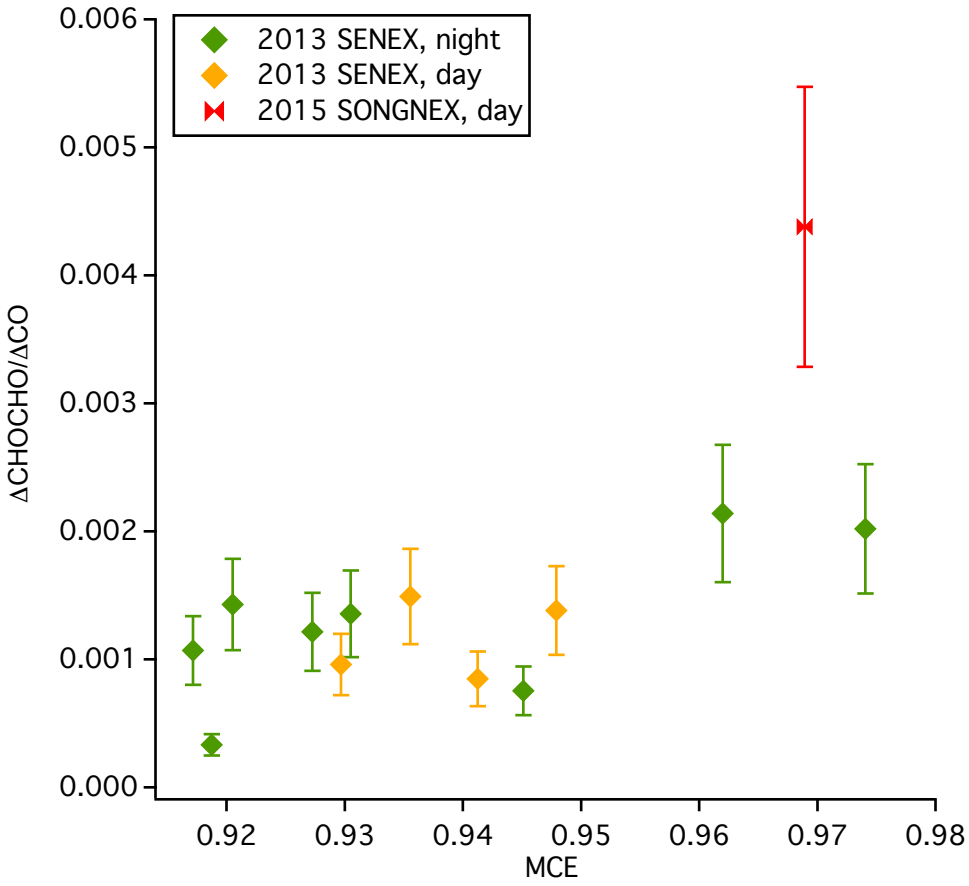

Figure S3: CHOCHO to CO NEMRs as a function of MCE.

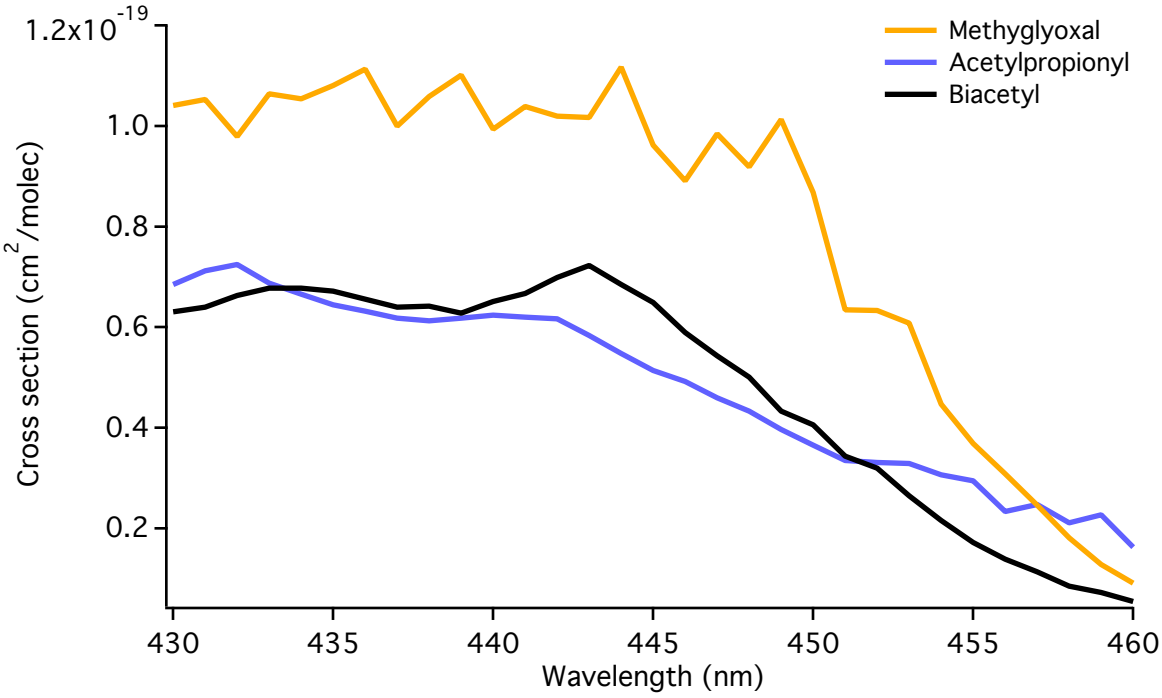

Figure S4: Absorption cross sections of substituted bicarbonyl compounds in the ACES retrieval window. The methylglyoxal cross section is from Meller et al.,[S5] the biacetyl cross section is from Horowitz et al.,[S6] and the acetylpropionyl cross section is from Messaadia et al.[S7]

Table S1: Times, locations, and NEMRs for the 2013 SENEX nighttime intercepts. Intercept Location is the position of the aircraft when it intercepted the plume.

Date	**Time (local)**	**Intercept Location**	**Intercept Altitude (m)**	**ΔCHOCHO: ΔCO NEMR**	**ΔCHOCHO: ΔHCHO NEMR**	**MCE**	**Notes**
2 July 2013	20:39	33 km SE of New Madrid, MO 36.335 N, 89.334 W	570	0.0014	0.043	0.93	
2 July 2013	20:55	29 km SE of New Madrid, MO 36.394 N, 89.304 W	700	0.0011	0.031	0.917	MCE possibly influenced by power plant CO_2
2 July 2013	20:58	35 km SE of New Madrid, MO 36.345 N, 89.256 W	690	0.0012	0.030	0.927	MCE possibly influenced by power plant CO_2
2 July 2013	21:00	29 km SSE of New Madrid, MO 36.333 N, 89.366 W	870	0.0008	0.016	0.945	
2 July 2013	21:05	35 km SW of New Madrid, MO 36.332 N, 89.766 W	870	0.0012	0.032		No CO_2 data
2 July 2013	21:16	28 km SE of New Madrid, MO 36.426 N, 89.291 W	975	0.0003	0.009	0.919	
2 July 2013	21:46	37 km SE of New Madrid, MO 36.338 N, 89.258 W	740	0.0014	0.037	0.92	MCE possibly influenced by power plant CO_2
2 July 2013	22:04	57 km SE of New Madrid, MO 36.151 N, 89.166 W	700	0.0016	0.038		No CO_2 data
2 July 2013	22:16	87 km SE of New Madrid, MO 35.976 N, 88.926 W	700	0.0020	0.042	0.974	
2 July 2013	22:25	67 km S of New Madrid, MO 35.969 N, 89.695 W	700	0.0021	0.042	0.962	

Table S2: Times, locations, and NEMRs for the 2013 SENEX daytime intercepts.

Date	**Time (local)**	**Intercept Location**	**Intercept Altitude (m)**	**ΔCHOCHO: ΔCO NEMR**	**ΔCHOCHO: ΔHCHO NEMR**	**MCE**	**Notes**
10 June 2013	11:51	On the Louisiana/Texas border, 110 km south of Shreveport, LA 31.528 N, 93.826 W	525	0.0009	0.027	0.941	
11 June 2013	16:27	70 km east of Birmingham, AL 33.488 N, 86.045 W	740	0.0015	0.038	0.936	
25 June 2013	11:52	55 km east of Shreveport, AL 32.569 N, 93.173 W	580	0.0010	0.031	0.93	
10 July 2013	11:58	10 km south of Goldsboro, NC 35.290 N, 77.990 W	510	0.0028	0.042		
10 July 2013	12:22	35 km southeast of Goldsboro, NC 35.105 N, 77.799 W	505	0.0014	0.025	0.948	Possibly from biomass burning power plant

Table S3: Times, locations, and NEMRs for the 2015 SONGNEX daytime intercepts.

Date	**Time (local)**	**Intercept Location**	**Intercept Altitude (m)**	**ΔCHOCHO: ΔCO NEMR**	**ΔCHOCHO: ΔHCHO NEMR**	**MCE**	**Notes**
19 March 2015	15:01	19 km south of Lake Okeechobee, FL 26.558 N, 80.807 W	555	0.0018	0.062		Likely burning sugarcane fields, no CO_2 data
20 April 2015	15:53	65 km west of Enid, OK 36.529 N, 98.597 W	850	0.0044	0.110	0.969	

References

(S1) Akagi, S. K.; Yokelson, R. J.; Wiedinmyer, C.; Alvarado, M. J.; Reid, J. S.; Karl, T.; Crounse, J. D.; Wennberg, P. O. Emission factors for open and domestic biomass burning for use in atmospheric models. *Atmospheric Chemistry and Physics* **2011**, *11*, 4039–4072, DOI: 10.5194/acp-11-4039-2011.

(S2) Yokelson, R. J.; Burling, I. R.; Gilman, J. B.; Warneke, C.; Stockwell, C. E.; de Gouw, J.; Akagi, S. K.; Urbanski, S. P.; Veres, P.; Roberts, J. M.; Kuster, W. C.; Reardon, J.; Griffith, D. W. T.; Johnson, T. J.; Hosseini, S.; Miller, J. W.; Cocker III, D. R.; Jung, H.; Weise, D. R. Coupling field and laboratory measurements to estimate the emission factors of identified and unidentified trace gases for prescribed fires. *Atmospheric Chemistry and Physics* **2013**, *13*, 89–116, DOI: 10.5194/acp-13-89-2013.

(S3) Gilman, J. B.; Lerner, B. M.; Kuster, W. C.; Goldan, P. D.; Warneke, C.; Veres, P. R.; Roberts, J. M.; de Gouw, J. A.; Burling, I. R.; Yokelson, R. J. Biomass burning emissions and potential air quality impacts of volatile organic compounds and other trace gases from fuels common in the US. *Atmospheric Chemistry and Physics* **2015**, *15*, 13915–13938, DOI: 10.5194/acp-15-13915-2015.

(S4) Stockwell, C. E.; Veres, P. R.; Williams, J.; Yokelson, R. J. Characterization of biomass burning emissions from cooking fires, peat, crop residue, and other fuels with high-resolution proton-transfer-reaction time-of-flight mass spectrometry. *Atmospheric Chemistry and Physics* **2015**, *15*, 845–865, DOI: 10.5194/acp-15-845-2015.

(S5) Meller, R.; Raber, W.; Crowley, J.; Jenkin, M.; Moortgat, G. The UV-visible absorption spectrum of methylglyoxal. *Journal of Photochemistry and Photobiology A: Chemistry* **1991**, *62*, 163–171, DOI: 10.1016/1010-6030(91)87017-P.

(S6) Horowitz, A.; Meller, R.; Moortgat, G. K. The UV-VIS absorption cross sections of the α-dicarbonyl compounds: pyruvic acid, biacetyl and glyoxal. *Journal of Photochemistry and Photobiology A: Chemistry* **2001**, *146*, 19–27, DOI: 10.1016/S1010-6030(01)00601-3.

(S7) Messaadia, L.; Dib, G. E.; Ferhati, A.; Chakir, A. UV-visible spectra and gas-phase rate coefficients for the reaction of 2,3-pentanedione and 2,4-pentanedione with OH radicals. *Chemical Physics Letters* **2015**, *626*, 73–79, DOI: 10.1016/j.cplett.2015.02.032.